The behaviour of alpha -quartz and pressure-induced SiO$_2$ glass under pressure: a molecular dynamical study

The behaviour of α-quartz and pressure-induced SiO$_2$ glass under pressure: a molecular dynamical study

M S Somayazulu†, Surinder M Sharma†, Nandini Garg†, S L Chaplot‡ and S K Sikka†

† High Pressure Physics Division, Bhabha Atomic Research Centre, Bombay 400 085, India
‡ Solid State Physics Division, Bhabha Atomic Research Centre, Bombay 400 085, India

Abstract. We have carried out extensive molecular dynamical calculations on α-quartz and pressure-induced glass and have related these to the experimental observations under static and shock pressure loading. In the crystalline quartz, densification and amorphization take place sharply around 20 GPa and are related to the changes in the Si coordination. The pressure-induced glass is considerably less compressible than the fused silica, showing a gradual change in the Si coordination, and is unlike the glass studied earlier by Tse, Klug and Le Page. However even this glass shows a densification, similar to that of quartz as well as fused silica. Retrieval of the four-coordinated state, in both cases, requires annealing at high temperatures. Just before amorphization of α-quartz, O atoms are still far from the recently proposed BCC packing.

1. Introduction

Over the last few years, numerous compounds have been shown to transform to the amorphous phase when subjected to static high pressures [1–3]. The material is amorphized under pressure due to the structural frustration in reaching the dense-packed high-pressure equilibrium phase. This is the result of unfavourable kinetics and is thermodynamically symbolized by a three-level diagram [1, 4, 5]. Evaluation of steric hindrances provides a reasonable quantitative estimate of the pressures of this transformation, irrespective of the nature of the underlying bonding in these materials [6]. There is growing evidence that the same transformation also takes place when these materials are subjected to shocks, even though the resulting microstructure may be different due to different strain loading rates and its uniaxial nature [4, 7, 8]. A Raman spectroscopic study of shock-recovered quartz suggests that the untransformed quartz is under tensile stress which requires that the resulting glass be of higher density than α-quartz [9]. Static high-pressure x-ray absorption experiments on isostructural GeO$_2$ indicate that the Ge–O bond length never reverts back to the original value after release of pressure from the amorphous phase [10]. It is possible that this is also the case for α-quartz. To have deeper insight into such atomic processes involved in this transformation, it is necessary to resort to detailed atomistic, such as molecular dynamical, calculations. Recently a few such calculations have helped considerably in achieving a better understanding of this transformation [11–15]. Understandably, most calculations have concentrated on SiO$_2$ since there is a large amount of experimental information available on this [7–9, 16–19] and also because of the availability of reliable pair potentials for this material [20, 21]. In this paper we present the results of our detailed molecular dynamics (MD) calculations on SiO$_2$ as a function of pressure and temperature. Because the pressure-induced amorphization is essentially a consequence of the compression of materials, we

would relate these to the experimental results; amongst others, to those for shock-recovered quartz. However, as we are not dealing with shock propagation in materials, the present calculation cannot provide details about the various lamellae observed in experiments [7, 8]. The experimental observations could be understood, to the extent that the recovered state is related to the locally equilibriated pressure–temperature state. Some of the results of the calculation have been presented earlier [12] and the present paper extends those results.

2. Molecular dynamical simulations

The MD simulations presented here have been carried out using a program which is based on the constant-volume method and has been described elsewhere [22]. Equations of motions were integrated by Verlet's algorithm [23] using a time step of 0.002 ps. The simulations as a function of pressure and temperature use the size and shape of the unit cell as variables. In the program the cell dimensions are determined by equating the internal stress to the external pressure. Our procedure is similar to that of Pawley and Thomas [24]. The starting atomic configuration is the crystallographic structure of α-quartz at ambient conditions. The temperature and hence the kinetic energy are slowly increased to a temperature of 300 K in about 10 ps. At each pressure and temperature the system is equilibriated for at least 100 ps. We have used the pair potentials derived by Tsuneyuki *et al* [20], obtained through first-principles many-body calculations for clusters which reproduce various equilibrium crystal structures of SiO_2. The bond angles and bond lengths calculated using this potential [12] agree very well with the accurate *ab initio* calculations of Chelikowski *et al* [25]. However, this potential has instabilities at very short Si–O and O–O distances which could be reached by crossing of the potential barriers due to high velocities at high temperatures (> 4000 K) [26]. In our case the time step chosen is small enough that even at the highest temperatures in our simulation (2300 K) the atoms do not reach these short distances. However the program has built-in error diagnostics to detect such a situation. Simulations were carried out using a periodic macrocell of 162 and 243 atoms with essentially similar results. The pressure was raised in steps of ~ 5 GPa except near the transition where finer steps were used. Simulations have been carried out under the following conditions:

(1) pressure loading of α-quartz up to about 80 GPa at 300 K;

(2) unloading of pressure from 25 GPa at 300 K;

(3) heating of the terminal state of (2) to well above melting point (up to 2300 K) and cooling back to 300 K;

(4) increase of the temperature of the phase at 15 GPa and increase of pressure at this elevated temperature; and

(5) pressure loading of the terminal phase of (3) to 100 GPa and unloading the pressure from 40 GPa.

Heating in step (3) was carried out in steps of 100 K/10 ps equilibrating at each temperature. The internal energy when plotted as a function of temperature shows a change of slope at ~ 2200 K, similar to what has been observed by Valle and Andersen [27], and this is interpreted as melting. The unit cell volume jumped back to $\sim 98\%$ of the starting volume of the crystalline phase at this temperature. This phase was quenched to 1800 K from 2300 K and annealed to equilibrium at each lowering of 500 K. This somewhat sharper cooling schedule was chosen to mimic the lowering of temperature during shock unloading.

The initial α phase of quartz, when subjected to high pressures, amorphizes at about 20 GPa, consistent with our earlier results [12]. The evolution of the amorphous phase

from the crystalline α phase is shown in figure 1. For the sake of clarity, only one layer of Si atoms has been plotted in this figure. Figure 1(a) shows the structure of α-quartz at 20 GPa, just before amorphization takes place. This configuration of atoms is similar to that suggested by Hazen *et al* [17] and therefore supports their suggestion that O atoms tend to close pack on approach of amorphization. However, our results indicate that the atomic configuration remains just short of their extrapolated state at the onset of amorphization. We also find that the O atomic positions are nowhere near the proposed [28] BCC packing at the transition pressure.
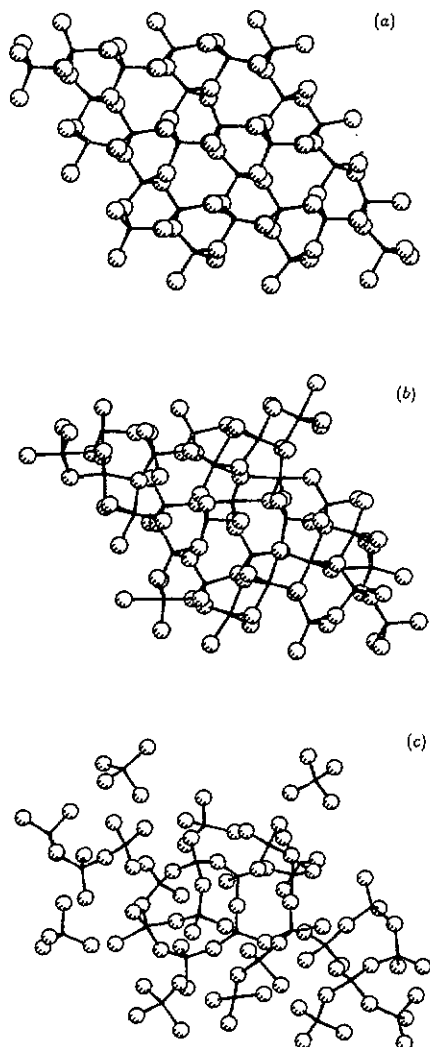

Figure 1. Projection down the c axis of α-quartz at different simulation conditions: (a) 50 ps before amorphization and (b) 50 ps after amorphization at $\sim$ 20 GPa, 300 K; (c) 0 GPa, 1100 K (after pressure release and subsequent high-temperature annealing). For the sake of clarity only one layer of Si atoms has been plotted. The large circles represent O atoms while the smaller circles are the Si atoms.

On amorphization, the open-ring configuration (six or three membered) of the crystalline phase becomes progressively distorted into a smaller ring structure with increasing pressure. This is in agreement with some of the earlier suggestions [29, 30]. However, a noteworthy result is the appearance of a tridymite-like six-membered ring configuration when the retrieved amorphous phase (from step 2) is heated to $\sim$ 1100 K to regain the four-coordinated

state. The difference in the ring configuration of this phase and the crystalline phase is that the six-membered ring is no longer an open structure, but is composed of smaller four-membered rings. In figure 2, we have shown the full structure just after amorphization has taken place at $\sim$ 21 GPa. Prior to amorphization the full structure, when projected along the c axis, is identical to that in figure 1(a). A new notable feature from figure 2 is the existence of a shear when seen along the original c axis. This shearing does not vanish even on further increase or on complete unloading of pressure. The crystalline order is destroyed in the basal plane. On the other hand, if the initial temperatures are kept higher than 750 K, we see that the shearing vanishes. Further, if the retrieved amorphous phase (after pressure unloading) is heated to temperatures higher than 1000 K, the order along the c axis is also destroyed and one obtains essentially a three-dimensional isotropic glass. However, this shearing does not vanish on heating the amorphous phase at higher than amorphization pressures, even if annealed up to 2300 K. The pressure of amorphization shows a very weak dependence on initial temperatures up to 1000 K, which is at variance with the experimental result [8] that the pressure of complete amorphization under shocks decreases with temperature. In view of our results, we feel that the temperature dependence of the pressure characterizing the completeness of transformation is essentially a kinetics effect.
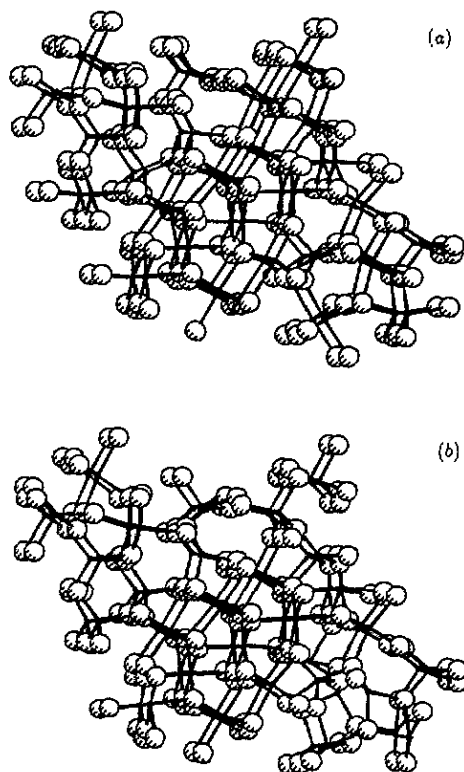

Figure 2. Projection down the c axis of the 162-atom macrocell used in the simulation studies: (a) 21 GPa, 300 K (during pressure loading); and (b) after pressure release from 25 GPa to 0 GPa at 300 K. The large circles represent O atoms while the smaller circles are the Si atoms.
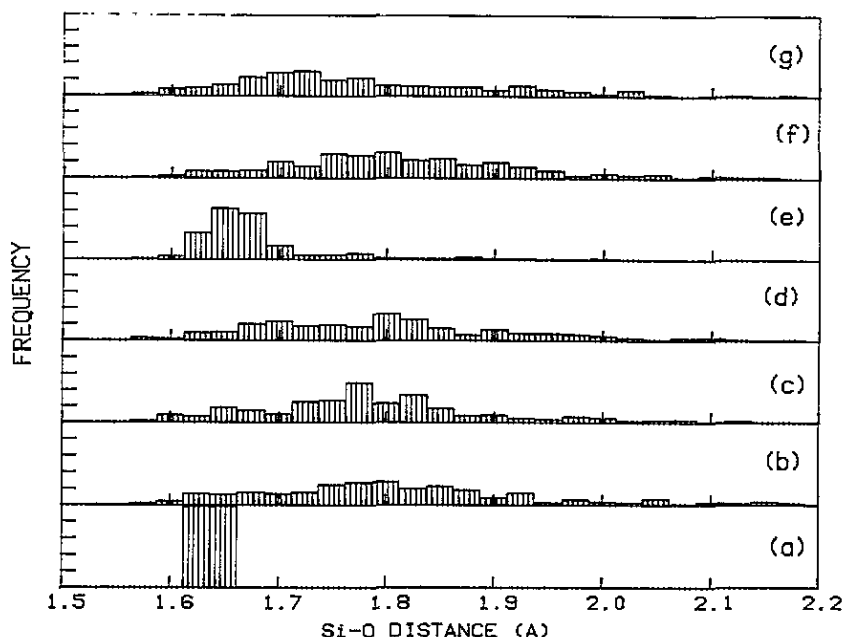
Figure 3. Frequency distribution of Si–O bonds in the interval 1.5–2.2 Å: (*a*) 15 GPa; (*b*) 21 GPa; (*c*) 42 GPa; (*d*) 0 GPa (all at 300 K); (*e*) 0 GPa, 1100 K; (*f*) 23 GPa, heated to 2300 K; (*g*) pressurized to 21 GPa at 950 K. (*a*)–(*c*) refer to increasing pressure while (*d*) and (*e*) are obtained from the pressure release.

Figure 3 shows the histogram of the distribution of O atoms within the bonding distance of 2.2 Å around an Si atom. Before the transformation Si–O bonds have a sharp distribution as expected. In the amorphous phase the distribution becomes spread out from ~ 1.6 Å to almost 2 Å. This indicates a substantial distortion of SiO₄ tetrahedra. At 40 GPa, the amorphous phase shows a higher percentage of bonds around 1.8 Å. On unloading the pressure, the distribution continues to be indicative of the amorphous phase. On raising the temperature of this retrieved glass to about 1100 K, there is some restoration of sharpness in the bond distribution. However, if the amorphous phase at 23 GPa is raised to temperatures as high as 2300 K, the histograms show only a small relaxation around 1.8 Å. On increase of the pressure for α-quartz at initial temperatures of about 1000 K, the resulting amorphous phase has a similar distribution as in figure 3(*b*), though with a small maximum around 1.7 Å.

The histograms of figure 3 are used to calculate the average Si–O bond length and this is shown in figure 4. Up to 20 GPa there is a small elastic compression of the Si–O bond length. The steep increase in the average Si–O distance to ~ 1.8 Å on amorphization indicates a weakening of the bond. This, as discussed below, results from the additional bonding of Si and O atoms once these come closer than the bonding distance, and supports the suggestion of Chelikowski *et al* [25]. Beyond the pressure of amorphization, the Si–O bond length decreases slowly. On unloading the pressure there is a large hysteresis and the bond length shows a steep decrease below 6 GPa, attaining a value of 1.665 Å at ~ 1 GPa. Even on increase of temperature up to ~ 1300 K, the bond length hardly shows any change.

So, the notable feature is that the average Si–O separation never reverts back to the starting value, which is very similar to what has been observed for GeO_2 under a similar pressure cycle [9].
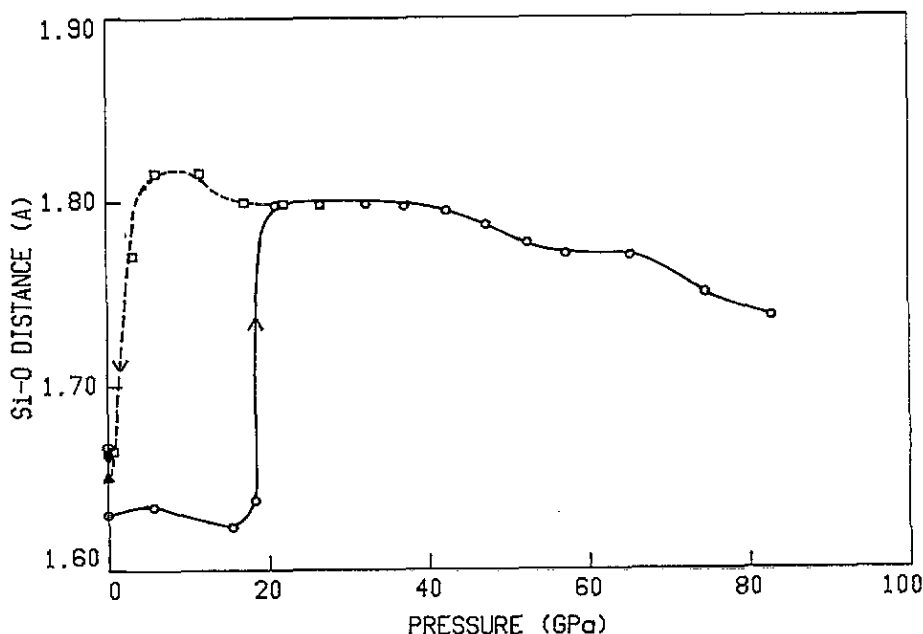

Figure 4. Average Si–O distance for the bonded atoms (< 2.2 Å) as a function of pressure. O represents pressure loading while □ represents unloading. The distances obtained after annealing the pressure-released phase at high temperatures are given as follows: hexagon, 500 K; *, 800 K; △, 1000 K; ▽, 1300 K and ▲, 2300 K. Hexagon, △ and ▽ are located close together on the vertical axis. The curves are meant to serve as guides to the eye.

In figure 5(a) we have shown the variation of average Si coordination under increasing and decreasing pressure. The change in the Si coordination is closely related to the behaviour of the average Si–O bond length. On increase of pressure the coordination changes abruptly and substantially beyond 20 GPa and attains a plateau at 5.8 between 25 GPa and 40 GPa. Full six coordination is approached slowly and is attained fully at ~ 65 GPa, and not at 80 GPa [11]. On decreasing pressure the coordination shows a large hysteresis loop and reduces steeply from 12 GPa to reach a final value of ~ 4.6, in slight disagreement with the results of Tse *et al* [14]. A fourfold coordination reverts back only on heating this phase to ~ 1000 K. Figure 5(b–d) shows how the fractions of Si atoms having four-, five- or sixfold coordination change on increase and decrease of pressure. Beyond 20 GPa, an increasingly larger number of Si atoms have coordination greater than four. For example, at 21 GPa, only 11% of Si atoms have four-, 15% have five- and 74% have sixfold coordination. On further increasing the pressure the number of fourfold coordinated atoms becomes vanishingly small while six coordination increases at the cost of four as well as five. On complete unloading of pressure only about half the Si atoms revert to four coordination while about one third retain fivefold coordination.
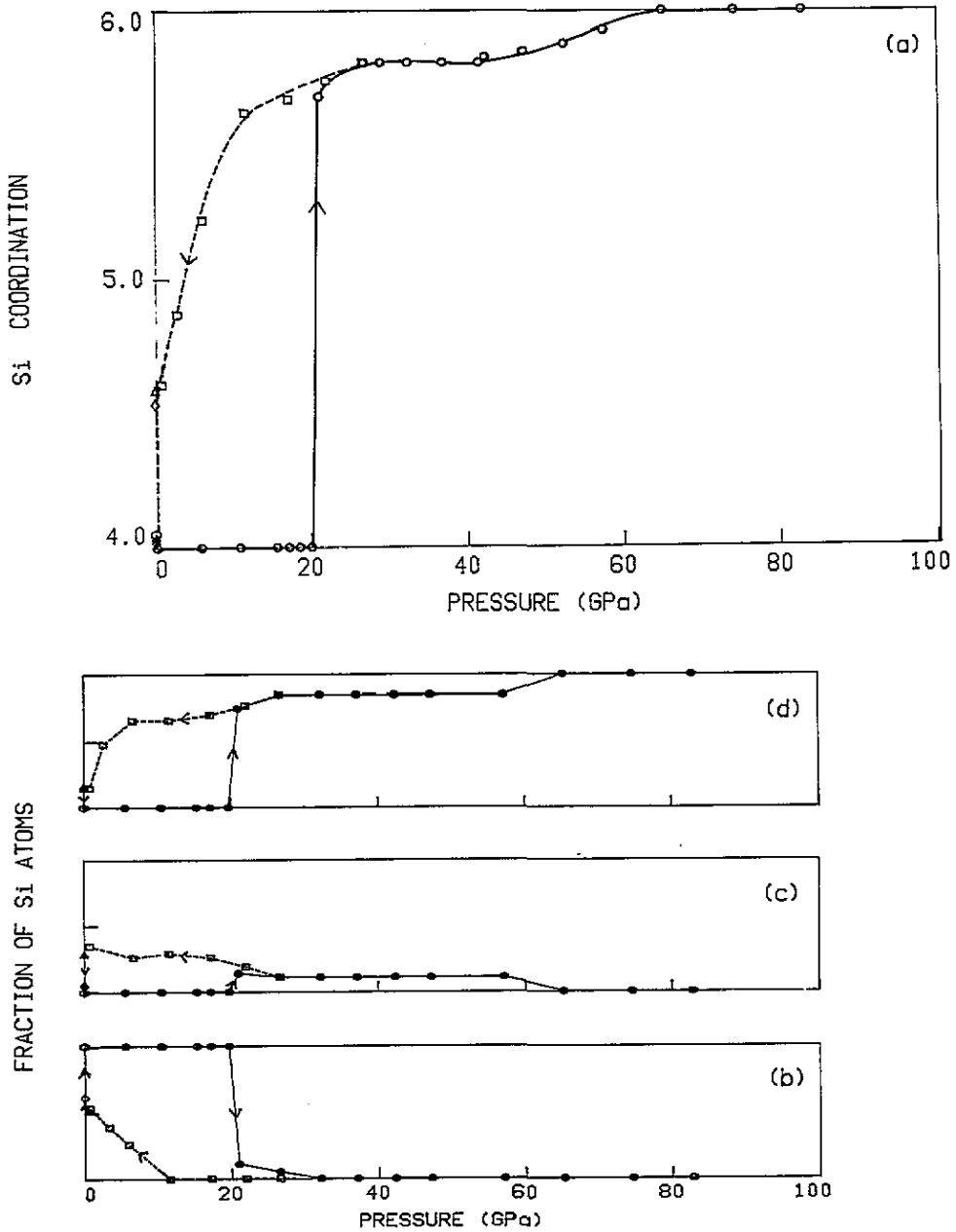
Figure 5. (a) Average Si coordination as a function of pressure. The fractions of (b) four-coordinated, (c) five-coordinated and (d) six-coordinated Si atoms have been plotted separately. O represents pressure loading and □ unloading. The coordination after annealing the pressure-released phase at high temperatures is indicated by Δ, 500 K; ◊, 800 K; and *, 1000 K. The curves are a guide to the eye.

The calculated P–V/V_0 is shown in figure 6. The agreement with experimental data of Levien *et al* [31] and of McWahan [32] in the crystalline phase is excellent. At higher
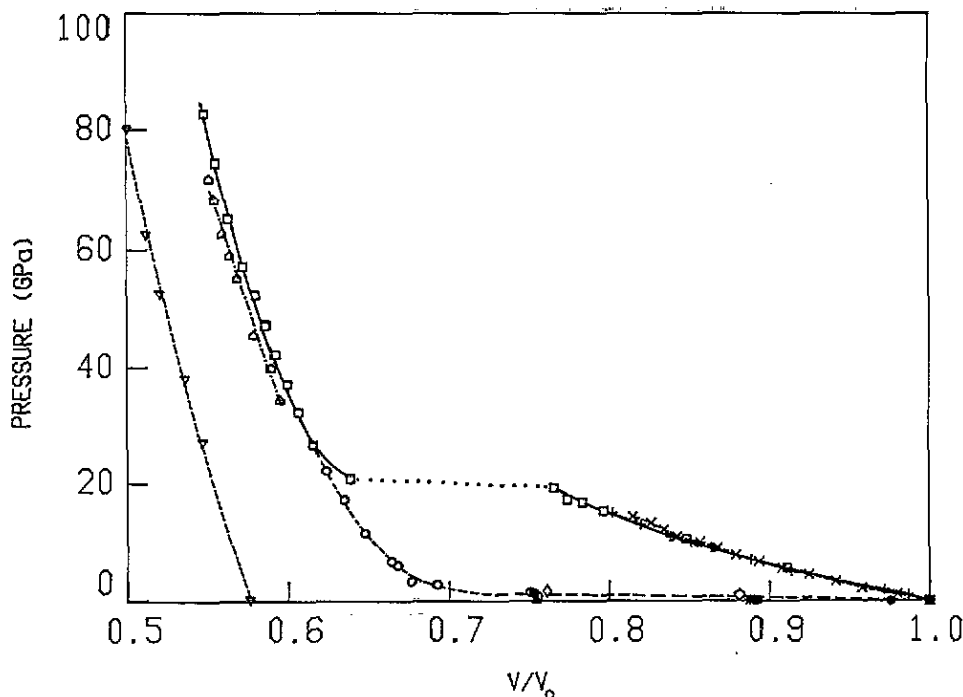
Figure 6. Calculated $P-V/V_0$ of α-quartz as a function of increasing ($\square$) and decreasing ($\bigcirc$) pressure. The experimental data for the crystalline phase under static pressures (< 15 GPa) of Levien *et al* ($\times$) [31] and McWahan ($+$) [32] are also shown for comparison. Shock data for pressures higher than 20 GPa for x-cut α-quartz (pentagons) are also shown [33]. The equation of state of stishovite [34] is shown by $\triangledown$. The data for the high-temperature thermal annealing of the pressure-released phase are shown by $\triangle$, 500 K; $\Diamond$, 800 K; (hexagons), 1000 K; *, 1300 K; $\oplus$, 1500 K and $\bullet$, 2300 K. The data obtained from [31–34] have been scaled with respect to the initial volume V_0 (120.75 Å^3) of our simulation studies. The curves are meant to be guides to the eye.

pressures the $P-V$ behaviour of the amorphous phase is very close to that of the shocked α-quartz [33]. Because of the phase transformation, it is difficult to construct an isotherm from shock data, but the agreement is highly suggestive of the shocked state also being amorphous. For comparison the calculated isotherm of stishovite is also shown [34]. The behaviour of the amorphous phase on unloading of pressure from 25 GPa is considerably different from the equation of state of fused SiO_2. In particular, the retrieved phase at 300 K continues to be the densified one at $V/V_0 \simeq 0.75$. This feature is related to the residual coordination of 4.6 and also the residual increase in the Si–O bond length mentioned above. This brings out the principal difference between the melt glass and the pressure-amorphized glass, despite the fact that recent high-resolution transmission electron microscopic studies indicate that there is no microstructural difference between the two amorphous phases [35]. An indirect confirmation of this is provided by the release wave in the shock experiments on x-cut quartz [36]. In fact the shock-unloading behaviour in quartz, as studied by Chhabildas [36], is very similar to that of figure 6. With the present pair potentials we revert to close to the starting volume ($V/V_0 \simeq 0.975$) only on annealing at 2300 K.
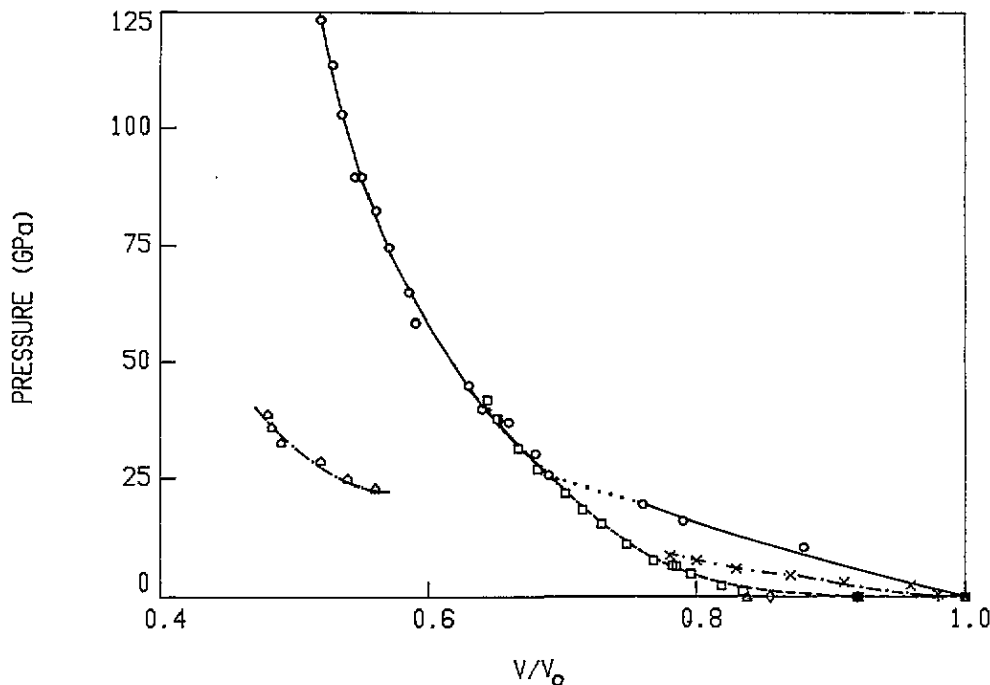
Figure 7. P–V/V_0 for the pressure-induced glass: $\bigcirc$ represents pressure loading while $\square$ represents unloading. The pressure-released phase was again subjected to thermal annealing at high temperatures shown by $\triangle$, 500 K; $\Diamond$, 800 K, *, 1000 K; and $+$, 1200 K. For comparison the experimental static pressure data ($\times$) of [38] and the shock data (pentagons) of [39] are also plotted, after scaling them to the initial volume V_0 (115.30 Å³) of our pressure-induced glass. The curves are meant to serve as guides to the eye.

3. Simulations of four-coordinated glass

Now we shall describe the results of MD calculations on the four-coordinated amorphous phase obtained after the pressure unloading from 25 GPa and subsequent annealing. As discussed above, the recovered pressure-amorphized phase was heated slowly to 2300 K. Although the four coordination of Si is realized at about 1000 K, volume and average Si–O distance relax only after heating beyond 2200 K, which is the melting point in our simulation. After annealing to equilibrium at 2300 K, the resulting phase was quenched to 1800 K and subsequently cooled according to the schedule given above. Therefore, this glass obtained after minimal heating is qualitatively different from the fused silica studied by Tse *et al* [14], which was prepared from melting cristabolite and quenching from a temperature of 7000 K. This study would hence serve a purpose in evaluating whether the response of pressure-generated glass is any different from the fused silica. This new glass was subjected to pressures of up to 100 GPa. The pressure-unloading behaviour was studied from ~ 50 GPa. P–V behaviour is shown in figure 7 and is compared with the experimental data of fused silica. The pressure-generated glass is far less compressible than the fused silica under both static [37] and shock compression [38]. The change in the Si coordination is shown in figure 8 and is similar to that of α-quartz except that the variations are relatively smooth. There is substantial coordination change around 25 GPa.
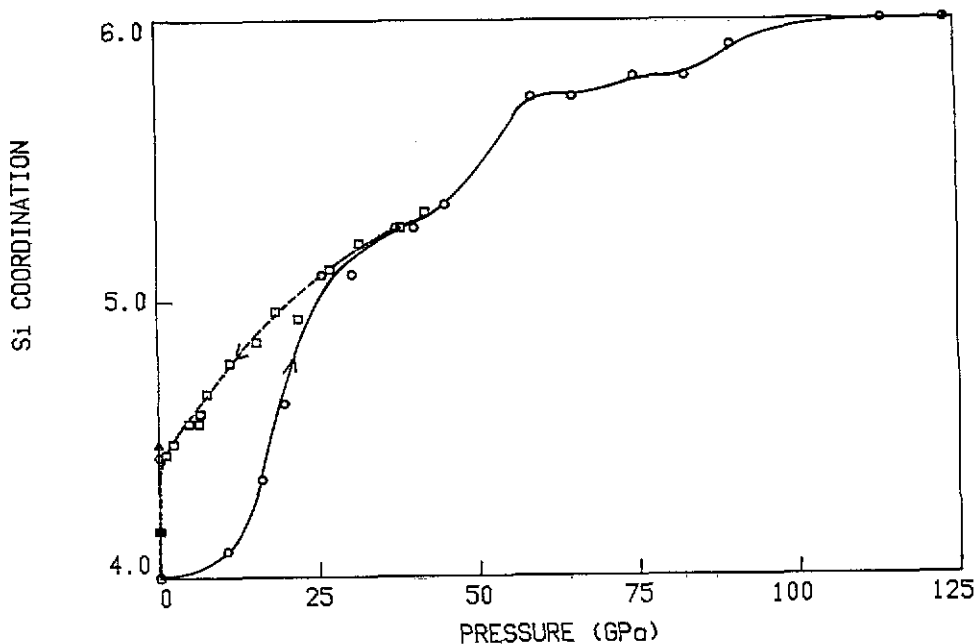
Figure 8. The variation of Si coordination in the pressure-induced glass as a function of pressure while pressure loading (O) and unloading (□). The coordination of the pressure-released phase at high temperatures is shown by △, 500 K; ◊, 800 K; and *, 1000 K. Complete reversion to four coordination takes place at 1200 K. The curves are guides to the eye.

The significant difference from the results for α-quartz is that here, around 25 GPa, the weighting of five and six coordinations is comparable. Only beyond 50 GPa does six-coordinated Si become dominant, and around 100 GPa the glass is fully six coordinated. In contrast, the glass studied by Tse *et al* shows six coordination at 30 GPa. On release of pressure we continue to see a permanent densification of about 16%, and the coordination equilibrates at ~ 4.5. The permanent densification is comparable to what has been calculated by Tse *et al* [14]. On annealing this retrieved phase at ~ 1200 K the amorphous phase is de-densified and four coordination reverts.

4. Discussions and conclusions

One of the interesting results of these MD calculations is the formation of compacted glass, which can be anisotropic or isotropic depending upon the heat treatment. For example, in static pressure experiments the retrieved amorphous phase is likely to be anisotropic unless deliberately annealed. However, in shock experiments there is always a possibility of shear zones and consequent higher temperatures [39]. So if the average bulk temperature on shock release is substantially higher than 1000 K, then the retrieved glass may revert to the four-coordinated state and will be isotropic, but if the residual temperature is considerably smaller than 1000 K, the resulting glass would be a compacted one of higher density. Alternatively one may obtain a distribution of coordination and density which reflects the temperature distribution. So the observation of two kinds of glass in microscopy experiments may not be

indicative of different origin, i.e., melt and solid–solid glass [8]. Further, Raman scattering experiments indicate the existence of tensile stress in the shock-retrieved quartz, implying the retention of higher-density glass [9]. This can be rationalized in terms of the arguments given above.

As we have already commented in the context of figures 1 and 2, the O movement just before amorphization is not substantial enough to be close to the suggested BCC phase [28]. Related to this is the suggestion that the principal driving mechanism of amorphization is the violation of the Born stability condition by the vanishing of the shear modulus B_3. We would like to bring into focus the fact that prior to the vanishing of B_3 (at 23 GPa), a zone boundary mode at $[\frac{1}{3}, \frac{1}{3}, 0]$ goes soft (around 19 GPa) [12]. In principle this could be the driving cause of making B_3 vanish. The atomic configuration just before amorphization is quite close to that suggested by Hazen *et al* [17], so the amorphization occurs when SiO_4 tetrahedra are compacted to almost the maximum degree permissible by the topology of the quartz structure, and results from the kinetic frustration of the evolution of Si coordination from four to six. The existence of fivefold coordination at the onset of amorphization symbolizes the frustration necessary for the process.

References

[1] Sikka S K 1992 *Recent Trends in High Pressure Research, Proc. XIII AIRAPT Int. Conf. on High Pressure Science and Technology (Bangalore, 1991)* ed A K Singh (New Delhi: Oxford & IBH) p 254; 1992 *Met. Mater. Processes* **3** 303

[2] Serghiou G C, Winters R R and Hammack W S 1992 *Phys. Rev. Lett.* **68** 3311

[3] Meade C and Jeanloz R 1990 *Geophys. Res. Lett.* **17** 1157

[4] Sikka S K and Sharma Surinder M 1992 *High Pressure Res.* **10** 675

[5] Johnson W L 1986 *Prog. Mater. Sci.* **30** 81

[6] Sikka S K and Sharma Surinder M 1992 *Curr. Sci.* **63** 317

[7] Ashworth J R and Schneider H 1985 *Phys. Chem. Miner.* **11** 249

[8] Gratz A J, Nellis W J, Christie J M, Brocious W, Swegle J and Cordier P 1992 *Phys. Chem. Miner.* **19** 261

[9] McMillan P F, Wolf G H and Lambert P 1992 *Phys. Chem. Miner.* **19** 71

[10] Itie J P, Polian A, Calas G, Petiau J, Fontaine A and Tolintino H 1989 *Phys. Rev. Lett.* **63** 398

[11] Tse J S and Klug D D 1991 *Phys. Rev. Lett.* **67** 3559

[12] Chaplot S L and Sikka S K 1993 *Phys. Rev.* B **47** 5710

[13] Tse J S 1992 *J. Chem. Phys.* **96** 5482

[14] Tse J S, Klug D D and Le Page Y 1992 *Phys. Rev.* B **46** 5933

[15] Binggeli N and Chelikowski J R 1992 *Phys. Rev. Lett.* **69** 220

[16] Hemley R J, Jephcoat A P, Mao H K, Ming L C and Manghnani M H 1988 *Nature* **334** 52

[17] Hazen R M, Finger L W, Hemley R J and Mao H K 1989 *Solid State Commun.* **72** 507

[18] Meade C, Hemley R J and Mao H K 1992 *Phys. Rev. Lett.* **65** 1387

[19] McNeil L E and Grimsditch M 1992 *Phys. Rev. Lett.* **68** 83

[20] Tsuneyuki S, Tsukada M, Aoki H and Matsui Y 1988 *Phys. Rev. Lett.* **61** 869
      Tsuneyuki S, Matsui Y, Aoki H and Tsukada M 1989 *Nature* **339** 209

[21] van Beast B W H, Kramer G J and van Santen R A 1990 *Phys. Rev. Lett.* **64** 1955

[22] Rao K R and Chaplot S L 1979 *Current Trends in Lattice Dynamics, Proc. IPA Seminar (Bombay, 1978)* ed K R Rao (Bombay: Indian Physics Association) p 589
      Chaplot S L 1986 *Curr. Sci.* **55** 949

[23] Verlet L 1967 *Phys. Rev.* **159** 98

[24] Pawley G S and Thomas G W 1982 *Phys. Rev. Lett.* **48** 410

[25] Chelikowski J R, King H E Jr, Troullier N, Martins J L and Glinnemann J 1990 *Phys. Rev. Lett.* **65** 3309

[26] Rustad J R and Yuen D A 1990 *Phys. Rev.* A **42** 2081

[27] Valle R G D and Andersen H C 1992 *J. Chem. Phys.* **97** 2682

[28] Binggeli N and Chelikowsky J R 1991 *Nature* **353** 344

[29] McMillan P, Piriou B and Couty R 1984 *J. Chem. Phys.* **81** 4234

[30] Hemley R J, Mao H K, Bell P M and Mysen B O 1986 *Phys. Rev. Lett.* **57** 747

[31] Levien L, Prewitt C T and Weidner D J 1980 *Am. Mineral.* **65** 920
[32] McWahan D B 1967 *J. Appl. Phys.* **38** 347
[33] Wackerle J 1962 *J. Appl. Phys.* **33** 922
[34] Yagi T, Tsuchida Y, Kusanagi S and Fukai Y 1990 *High Pressure Res.* **5** 699
[35] Winters R R, Garg A and Hammack W S 1992 *Phys. Rev. Lett.* **69** 3751
[36] Chhabildas L C 1986 *Shock Waves in Condensed Matter* ed Y M Gupta (New York: Plenum) p 601
[37] Meade C and Jeanloz R 1987 *Phys. Rev.* B **35** 236
[38] Marsh S P 1980 *LASL Shock Hugoniot Data* (Berkeley, CA: University of California Press)
[39] Grady D E 1980 *J. Geophys. Res.* **85** 913